

Supplementary Materials for

Chemical genomic analysis of GPR35 signaling

Heidi (Haibei) Hu^{a,§}, Huayun Deng^a, Shizhang Ling^{a,§§}, Haiyan Sun^{a,§§§},

Terry Kenakin^b, Xinmiao Liang^c, Ye Fang^{a,*}

^aBiochemical Technologies, Science and Technology Division, Corning Incorporated, Corning, NY 14831, USA

^bDepartment of Pharmacology, University of North Carolina School of Medicine, Chapel Hill, NC 27599, USA

^cKey Laboratory of Separation Science for Analytical Chemistry, Dalian Institute of Chemical Physics, Chinese Academy of Sciences, Dalian, Liaoning, China

[§] Current address: Medical Laboratory Science, Jefferson College of Health Science, Roanoke, VA 24013, USA

^{§§} Current address: Department of Medicine, Johns Hopkins University, Baltimore, MD, USA

^{§§§} Current address: Laboratory for Inflammation and Cancer, Biodesign Institute, Arizona State University, Tempe, Arizona

* Correspondence to: fangy2@corning.com

This PDF file includes:

- Fig. S1. Intra-plate data normalization for shRNA hit identification.
- Fig. S2. Characterization of GPR35 signaling pathway in HT-29 cells.
- Fig. S3. Pathway deconvolution of the DMR of zaprinast.
- Fig. S4. Impact of different compounds on the EGFR tyrosine kinase activity.
- Fig. S5. Effects of GPR35 agonist-treatment on HIF-1 α protein levels in serum starved HT-29 cells under normoxic condition.
- Fig. S6. Kinase network for resulting in resensitization of cells.
- Table S1. Excel data summarizing DNA microarray data and genes that gave rise to intensity greater 100 RFU under at least one treatment condition and displayed at least two fold changes in expression level.
- Table S2. The gene names, shRNA clones, and robust z-scores for the kinase hits identified for the early (10 min post stimulation) and late (50 min) events of the YE210 DMR.
- Table S3. The gene names, shRNA clones, and robust z-scores for a small set of kinase hits identified, where at least two shRNAs for the specific kinase altered the YE210 DMR by ≥ 2 MAD (median absolute deviation), but with opposite directions.

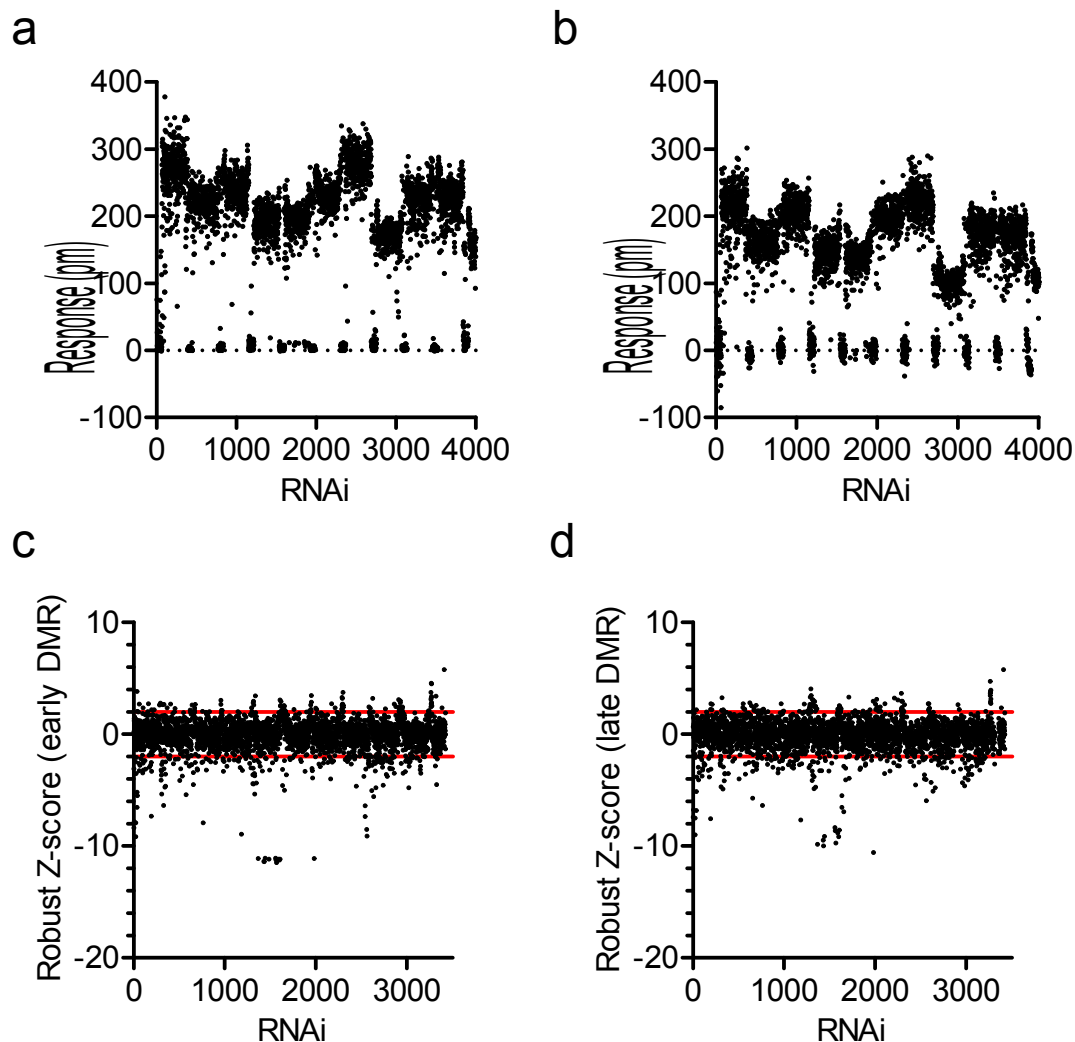


Fig. S1.

Intra-plate data normalization for shRNA hit identification. (a,b) The DMR amplitude, as indicated by response in picometer, Response (pm), at 10 min (a) or 50 min (b) post stimulation with YE210 as a function of shRNA treatment. (c,d) The robust z-score, a z-score not adversely affected by outliers, was calculated using $[(\text{experimental data} - \text{median}) / \text{median absolute deviation (MAD)}]$ and plotted as a function of each shRNA treatment, based on the DMR amplitude at 10 min (c) or 50 min (d) post stimulation with YE210. Here, an intra-plate normalization approach was applied (see Methods).

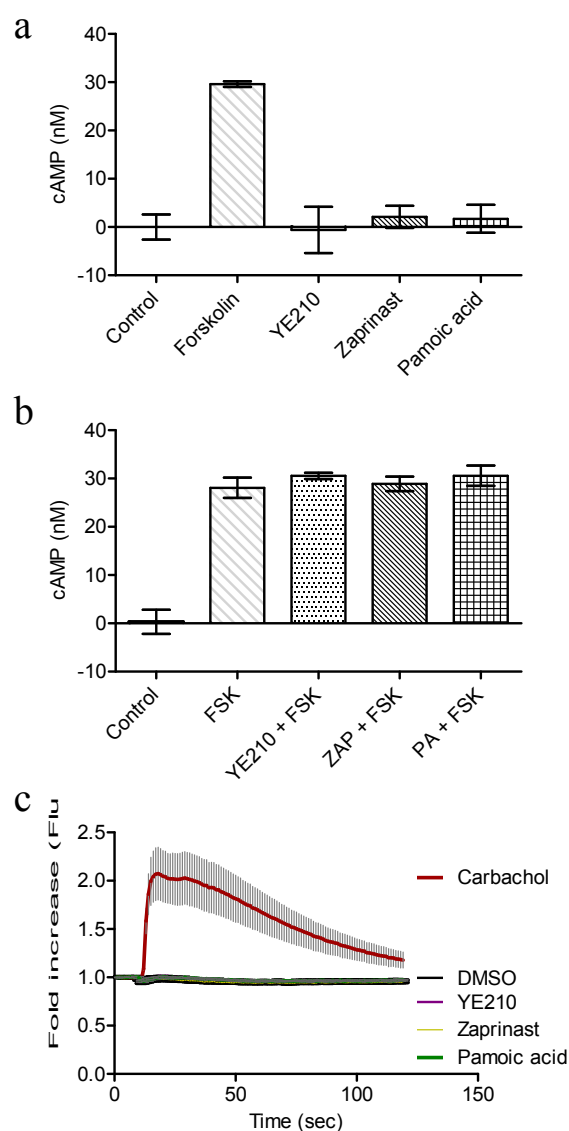


Fig.S2

Characterization of GPR35 signaling pathway in HT-29 cells. (a) cAMP

concentration as a function of compounds, each at 20 μ M. Cells were stimulated with each compound at 20 μ M for 30 min. (b) cAMP concentration as a function of compounds. Cells were stimulated for 30 min with 0.5 μ M forskolin (FSK) in the absence or presence of a GPR35 agonist, each at 20 μ M. (c) Fluo-4 Direct™ calcium assay signals, real-time fluorescence emission ratios, of three GPR35 agonists as well as carbachol, each at 10 μ M. Carbachol is an agonist for the endogenous G_q -coupled muscarinic M3 receptor in HT29, and used as the positive control. The data represent mean \pm standard deviation of 4 replicates for (a to c). These results suggest that three agonists tested, pamoic acid (PA), YE210, and zaprinast (ZAP), all were inactive in increasing cAMP (a), decreasing the forskolin-elevated cAMP (b), or causing Ca^{2+} mobilization (c).

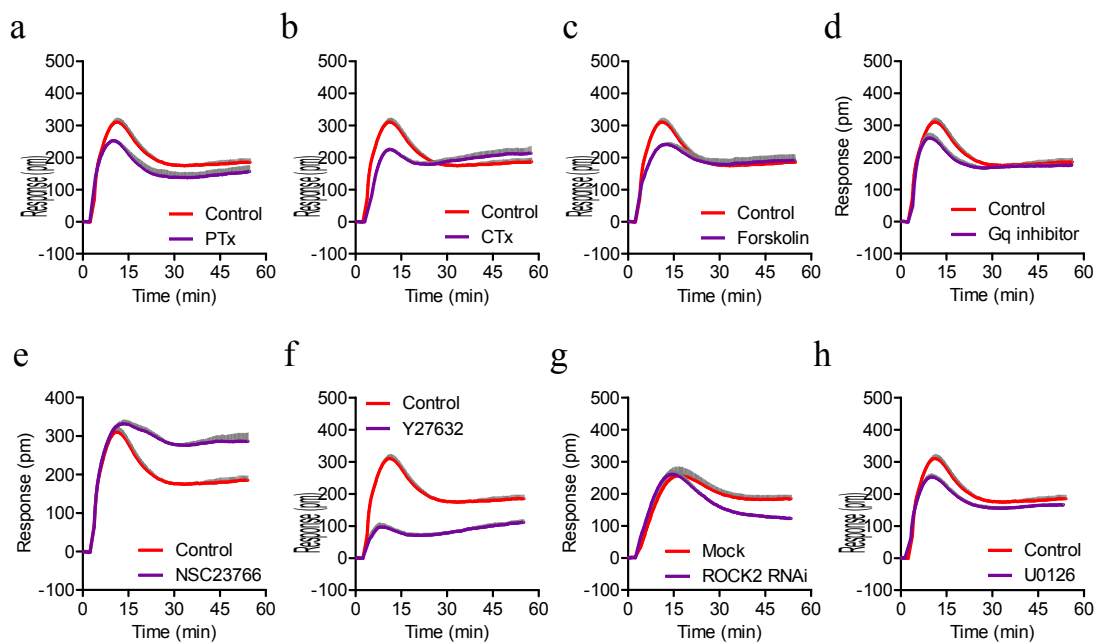


Fig. S3

Pathway deconvolution of the DMR of zaprinast. (a-h) The DMR of zaprinast in HT29 cells without (Control) or with pretreatment by 100 ng/ml pertussis toxin (PTx) (**a**); 400 ng/ml cholera toxin (CTx) (**b**); 10 μ M forskolin (**c**); 1 μ M FR900359 (G_q inhibitor) (**d**); 25 μ M NSC23766 (**e**); 10 μ M Y27632 (**f**); one ROCK2 siRNA (**g**); 10 μ M U0126 (**h**). In (**a-h**), data represents mean + standard deviation, $N=4$ (2 independent measurements, each in duplicate). The standard deviation is shown in gray.

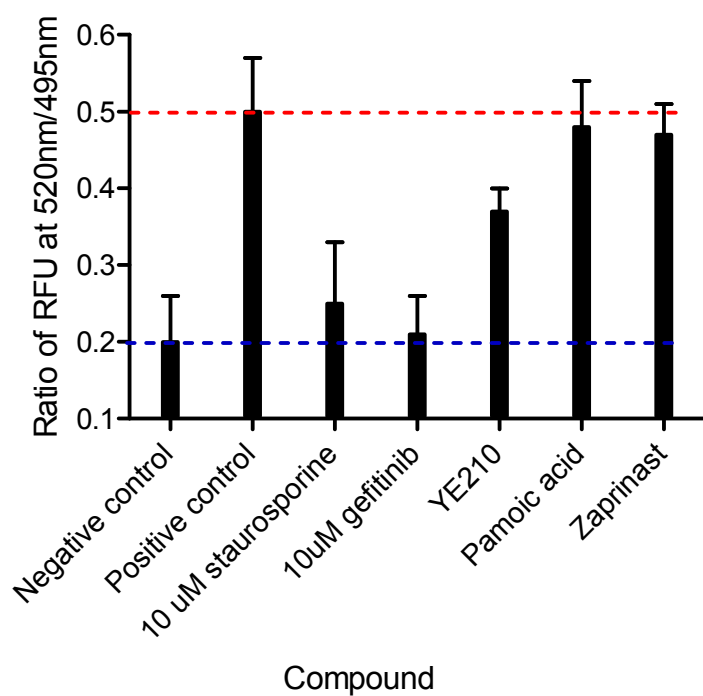


Fig. S4.

Effects of different compounds on EGFR tyrosine kinase activity. All compounds were assayed at 25 μ M, except for the two control compounds (staurosporine and Iressa) whose concentrations were indicated in the graph. Negative control: no EGFR kinase. Positive control: 50ng/ml EGFR plus 0.1 μ M the substrate as recommended by the supplier. Data are representative of three independent experiments.

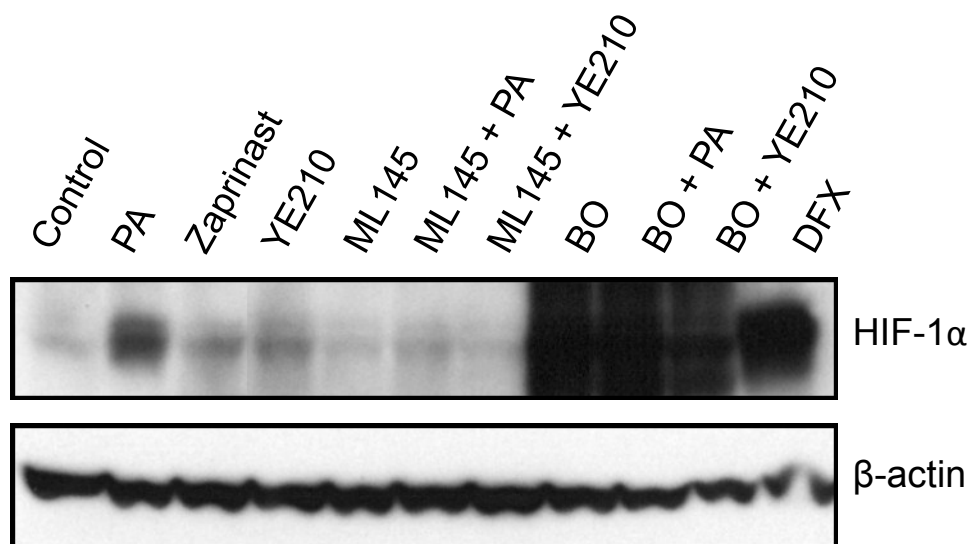


Fig. S5.

Effects of GPR35 agonist-treatment on HIF-1 α protein levels in serum starved HT-29 cells under normoxic condition. The concentrations of compounds were: 10 μ M pamoic acid (PA), 10 μ M zaprinast, 10 μ M YE210, 10 μ M ML145, 1 μ M bortezomib (BO), or 10 μ M deferoxamine mesylate (DFX). Both BO and DFX were used as the positive controls. Whole cell lysates were prepared at 5 hours post-treatment and HIF-1 α protein levels were determined by immunoblotting. Sample integrity was confirmed by immunoblotting for the β -actin as a control. Data are representative of three independent experiments.

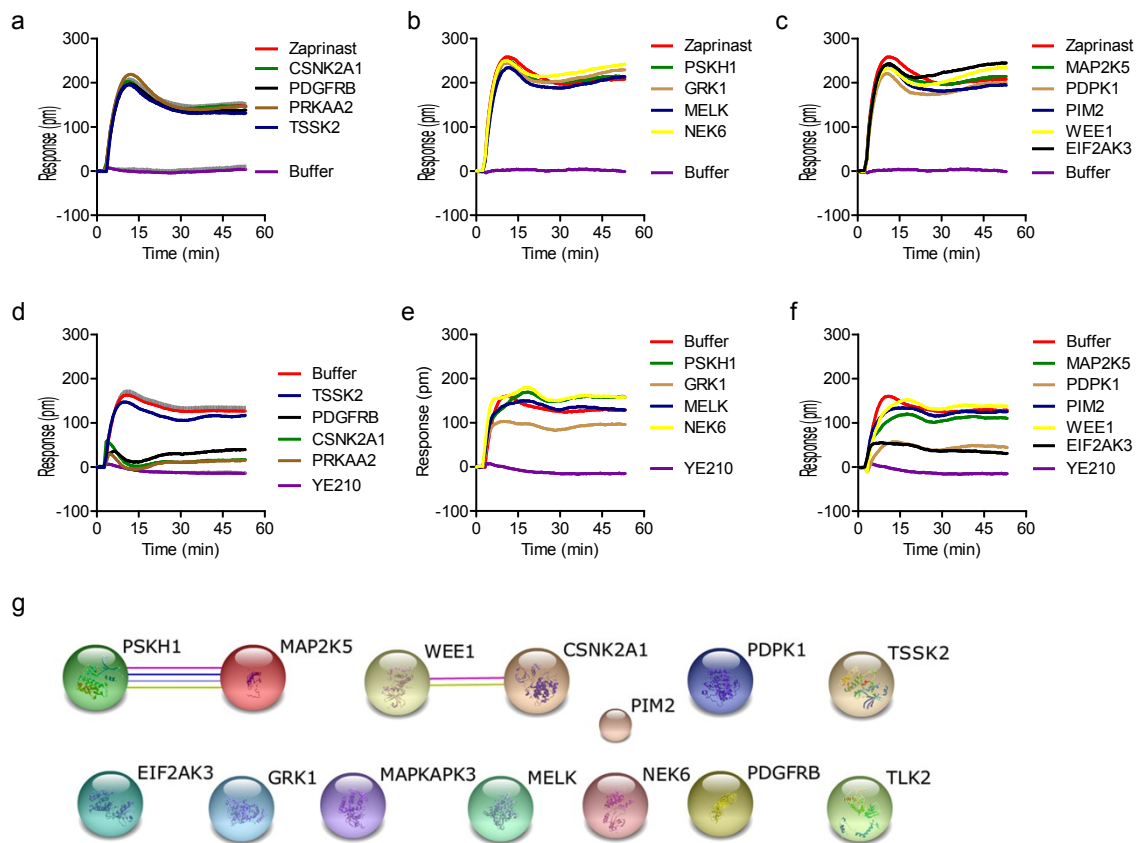


Fig. S6.

Kinase network for resulting in resensitization of cells. Here, the cells were treated with specific shRNAs, followed by stimulation with 1 μ M YE210 for 1 hour, and then 1 μ M zaprinast for another hour. Hits were selected based on that after shRNAi knockdown, cells gave rise to a DMR of YE210 comparable to the mock treated cells, but still responded to the subsequent stimulation with zaprinast. The network was generated using STRING 10. Connecting lines are color coded by the type of evidence used to build the network (details can be found in <http://string-db.org/>). Unconnected hits were also listed. GO enrichment analysis suggests that cytoskeleton organization (GO term 0007010), and response to stress (GO term 0006950) played important roles in the resensitization. Among these kinases, seven of them (MAP2K5, MELK, EIF2AK3, NEK6, MAPKAPK3, TLK2, WEE1) are known to involve in cell response to stress. Furthermore, five kinases, including TSSK2, PSKH1, MAP2K5, TLK2, and NEK6, are known to associate with cytoskeleton, while three (TSSK2, PSKH1, NEK6) are linked to microtubule organizing center, three (TSSK2, PDPK1 and PDGFRB) are linked to cytoplasmic membrane-bounded vesicle. Although these results have not been validated yet, these findings suggest a possibility that these kinases, at least in part, are involved the cellular mechanisms for GPR35 desensitization and resensitization process.

Table S2.

The gene names, shRNA clones, and robust z-scores for the kinase hits identified for the early (10 min post stimulation) and late (50 min) events of the YE210 DMR. These hits were identified when at least two shRNA clones for a single kinase within the library altered the YE210 DMR by ≥ 2 MAD (median absolute deviation); that is, a robust z-score of ≥ 2 or ≤ -2 . Results showed that there were 99 kinases in total, among which 42 were specific to the early DMR, 26 specific to the late DMR, and 32 common to both events. For the early DMR, there were 46 kinases whose knockdown decreased the DMR, and 27 kinases whose knockdown potentiated the DMR. On the other hand, for the late DMR, there were 35 kinases whose knockdown decreased the DMR, and 23 whose knockdown potentiated the DMR.

Gene name	shRNA clone	Early DMR Robust z-score	Late DMR robust z-score
AAK1	NM_014911.x-969s1c1	-2.9	-1.6
AAK1	NM_014911.2-2971s1c1	-2.0	-1.7
ABL1	NM_005157.x-3369s1c1	-2.5	-2.8
ABL1	NM_005157.3-1127s1c1	-2.0	-1.5
ABL1	NM_005157.2-1226s1c1	-0.6	-2.6
ACVR1B	NM_020328.x-783s1c1	-1.8	-3.5
ACVR1B	NM_020328.x-480s1c1	-1.1	-3.1
AKT1	NM_005163.1-1694s1c1	-2.4	-1.3
AKT1	NM_005163.x-1044s1c1	-2.0	-1.9
AKT3	NM_005465.3-437s1c1	-5.6	-5.1
AKT3	NM_005465.3-280s1c1	-2.4	-0.8
ALPK1	NM_001102406.1,NM_025144.3	-3.9	-2.0
ALPK1	NM_001102406.1,NM_025144.3	-3.3	-2.3
ALPK1	NM_001102406.1,NM_025144.3	-3.1	1.2
ATM	NM_000051.2-9380s1c1	2.0	1.8
ATM	NM_000051.2-9426s1c1	2.7	1.7
AURKB	NM_004217.x-883s1c1	-3.5	-4.3
AURKB	NM_004217.x-468s1c1	-3.1	-2.9
BCKDK	NM_005881.x-681s1c1	3.1	4.7
BCKDK	NM_005881.x-850s1c1	3.7	3.7
BLK	NM_001715.2-1626s1c1	-2.4	-2.1
BLK	NM_001715.x-261s1c1	-2.4	-2.6
BMPR1A	NM_004329.x-880s1c1	-2.6	-2.4
BMPR1A	NM_004329.2-2082s1c1	-2.6	-1.6
BMPR2	NM_001204.x-1962s1c1	-7.9	-7.5
BMPR2	NM_001204.x-488s1c1	-2.5	-1.8
BRD2	NM_005104.2-3578s1c1	1.5	2.0
BRD2	NM_005104.2-2059s1c1	1.7	2.3
BRD2	NM_005104.2-3720s1c1	1.4	2.4
BRDT	NM_001726.1-1632s1c1	1.6	2.5

BRDT	NM_001726.1-2117s1c1	2.0	1.1
BRDT	NM_001726.1-629s1c1	2.5	2.1
BUB1B	NM_001211.x-3346s1c1	-3.5	-2.1
BUB1B	NM_001211.x-521s1c1	-2.1	-1.0
CAMK2A	NM_171825.x-394s1c1	2.8	2.8
CAMK2A	NM_171825.x-1181s1c1	3.4	3.1
CAMK2A	NM_171825.x-1116s1c1	4.5	3.9
CAMK2B	NM_001220.x-2338s1c1	-6.5	-5.1
CAMK2B	NM_001220.x-1815s1c1	-5.2	-6.8
CAMK2G	NM_001222.x-2251s1c1	2.0	1.1
CAMK2G	NM_001222.x-279s1c1	2.7	1.4
CAMKK1	NM_172207.x-1434s1c1	-3.3	-3.1
CAMKK1	NM_172207.x-578s1c1	-2.3	-2.4
CAMKV	NM_024046.x-910s1c1	-2.8	-1.3
CAMKV	NM_024046.x-346s1c1	-2.0	-2.7
CDC2L1	NM_001787.1-2043s1c1	1.8	2.0
CDC2L1	NM_001787.1-511s1c1	1.5	2.0
CDC2L1	NM_001787.1-2259s1c1	1.6	2.2
CDC2L1	NM_001787.1-1490s1c1	2.1	2.3
CDC2L1	NM_001787.1-1156s1c1	2.9	1.9
CDC2L6	NM_015076.x-1837s1c1	-3.5	-2.5
CDC2L6	NM_015076.x-639s1c1	-2.4	-1.2
CDK3	NM_001258.x-1097s1c1	-3.3	-4.1
CDK3	NM_001258.x-618s1c1	-0.9	-2.0
CDK4	NM_000075.x-258s1c1	-9.2	-9.0
CDK4	NM_000075.2-818s1c1	-2.5	-1.6
CDK5	NM_004935.2-954s1c1	-1.9	-2.8
CDK5	NM_004935.2-208s1c1	-0.6	-2.1
CDK5	NM_004935.2-335s1c1	-1.8	-2.1
CDK6	NM_001259.5-4765s1c1	-3.8	-3.0
CDK6	NM_001259.3-1297s1c1	-0.8	-2.3
CDK9	NM_001261.2-1094s1c1	-2.6	-0.1
CDK9	NM_001261.2-858s1c1	-2.3	0.6
CDKL1	NM_004196.3-433s1c1	-11.2	-8.6
CDKL1	NM_004196.3-706s1c1	-11.1	-8.3
CHEK1	NM_001274.x-508s1c1	-3.5	-2.3
CHEK1	NM_001274.2-1196s1c1	-2.5	0.0
CLK1	NM_004071.x-1435s1c1	-5.3	-4.7
CLK1	NM_004071.x-1746s1c1	-3.2	-2.8
CLK1	NM_004071.x-762s1c1	-2.7	-2.2
CLK4	NM_020666.x-1413s1c1	2.1	1.1
CLK4	NM_020666.x-661s1c1	2.1	0.8
CSNK1G1	NM_022048.x-1348s1c1	-2.2	-3.0
CSNK1G2	NM_001319.5-521s1c1	-2.4	-0.8
DDR1	NM_001954.x-1857s1c1	-2.9	-3.2
DDR1	NM_001954.x-1358s1c1	-0.1	-2.1

DYRK3	NM_003582.x-658s1c1	-2.5	2.2
DYRK3	NM_003582.2-1880s1c1	-2.4	-3.9
DYRK4	NM_003845.x-1755s1c1	-4.7	-3.5
DYRK4	NM_003845.1-1342s1c1	-2.1	-1.3
EIF2AK2	NM_002759.x-474s1c1	2.0	2.8
EIF2AK2	NM_002759.x-1409s1c1	2.2	1.0
EPHA3	NM_005233.3-1787s1c1	2.1	-0.1
EPHA3	NM_005233.3-2263s1c1	2.2	0.7
EPHA3	NM_005233.3-301s1c1	2.3	0.5
EPHA3	NM_005233.3-1442s1c1	2.6	1.5
EPHA5	NM_004439.3-1346s1c1	2.0	0.8
EPHA5	NM_004439.3-3190s1c1	2.5	0.8
EPHA7	NM_004440.2-1859s1c1	2.0	0.2
EPHA7	NM_004440.2-3052s1c1	2.1	0.8
ERBB3	NM_001982.1-1904s1c1	2.7	1.1
ERBB3	NM_001982.1-2653s1c1	3.8	1.7
FER	NM_005246.x-1193s1c1	0.7	2.5
FER	NM_005246.x-883s1c1	0.5	2.7
FES	NM_002005.x-1641s1c1	-3.7	-2.3
FES	NM_002005.x-1875s1c1	-3.3	-2.0
FGFR1	NM_000604.x-2463s1c1	-1.1	-2.6
FGFR1	NM_000604.2-3436s1c1	-1.6	-2.4
GAK	NM_005255.1-4112s1c1	-0.4	-2.2
GAK	NM_005255.x-4100s1c1	-0.4	-2.2
GRK7	NM_139209.x-1781s1c1	-1.9	-3.3
GRK7	NM_139209.x-1725s1c1	-1.5	-2.1
IGF1R	NM_000875.2-2427s1c1	0.2	-2.8
IGF1R	NM_000875.2-4308s1c1	0.5	-2.0
IRAK1	NM_001569.x-2188s1c1	-7.3	-7.6
IRAK1	NM_001569.x-1049s1c1	-3.3	-3.1
IRAK1	NM_001569.3-1603s1c1	-0.1	-2.0
ITK	NM_005546.3-933s1c1	-2.2	-2.5
ITK	NM_005546.x-614s1c1	-1.6	-2.1
JAK1	NM_002227.x-849s1c1	-11.4	-9.5
JAK1	NM_002227.1-2927s1c1	-2.7	-1.6
JAK1	NM_002227.1-3336s1c1	-2.4	-0.3
JAK1	NM_002227.1-1148s1c1	-2.1	-1.7
LIMK1	NM_002314.x-3140s1c1	-3.6	-3.5
LIMK1	NM_002314.2-980s1c1	-2.4	-0.2
MAP2K3	NM_002756.x-1036s1c1	2.1	0.7
MAP2K3	NM_002756.x-826s1c1	2.1	0.8
MAP3K6	NM_004672.x-1039s1c1	1.7	3.1
MAP3K6	NM_004672.x-1283s1c1	2.8	3.1
MAP3K6	NM_004672.x-832s1c1	2.9	2.7
MAP3K9	NM_033141.2-749s1c1	-3.4	-4.6
MAP3K9	NM_033141.2-2603s1c1	-1.9	-2.6

MAPK14	NM_001315.x-3701s1c1	-2.4	-3.1
MAPK14	NM_139012.x-877s1c1	-1.0	-2.2
MARK4	NM_031417.2-2010s1c1	2.0	1.0
MARK4	NM_031417.2-2431s1c1	2.2	-0.4
MARK4	NM_031417.2-261s1c1	2.2	-0.7
MARK4	NM_031417.2-351s1c1	3.5	-0.7
MELK	NM_014791.2-1805s1c1	2.8	1.0
MELK	NM_014791.2-413s1c1	3.0	1.1
MET	NM_000245.2-2829s1c1	2.3	2.3
MET	NM_000245.1-2037s1c1	2.7	2.1
MET	NM_000245.1-1190s1c1	3.2	3.0
MINK1	NM_015716.2-2483s1c1	2.3	0.5
MINK1	NM_015716.2-1042s1c1	2.5	0.6
MKNK1	NM_003684.3-1404s1c1	2.2	1.0
MKNK1	NM_003684.3-284s1c1	2.3	0.1
MLKL	NM_152649.1-916s1c1	-7.4	-4.0
MLKL	NM_152649.x-1935s1c1	-2.2	-2.3
MLKL	NM_152649.1-1269s1c1	-1.1	-2.2
MST1R	NM_002447.x-609s1c1	-11.4	-10.0
MST1R	NM_002447.1-831s1c1	-3.1	1.1
NTRK2	NM_006180.x-2123s1c1	-2.6	-3.0
NTRK2	NM_006180.3-5300s1c1	-2.5	0.9
PAK4	NM_005884.x-1093s1c1	2.5	3.5
PAK4	NM_005884.x-285s1c1	2.7	3.8
PAK4	NM_005884.x-1540s1c1	2.7	2.9
PAK4	NM_005884.x-463s1c1	3.3	2.8
PAK4	NM_005884.x-1335s1c1	4.6	3.9
PDK2	NM_002611.x-834s1c1	1.7	4.0
PDK2	NM_002611.x-158s1c1	2.0	3.5
PDK2	NM_002611.x-803s1c1	2.4	2.0
PFTK1	NM_012395.x-416s1c1	0.6	2.1
PFTK1	NM_012395.x-1166s1c1	0.8	2.1
PFTK1	NM_012395.x-456s1c1	1.7	4.0
PHKG1	NM_006213.2-181s1c1	2.5	2.4
PHKG1	NM_006213.2-170s1c1	3.1	2.6
PIM1	NM_002648.2-1530s1c1	1.4	2.2
PIM1	NM_002648.2-528s1c1	2.5	2.7
PLK4	NM_014264.x-433s1c1	1.3	2.5
PLK4	NM_014264.2-2974s1c1	2.0	2.9
PLK4	NM_014264.2-1087s1c1	2.4	1.8
PLK4	NM_014264.2-3108s1c1	2.5	1.7
PRKACB	NM_002731.2-1710s1c1	-5.0	-4.3
PRKACB	NM_002731.2-523s1c1	-2.8	-2.4
PRKACB	NM_002731.x-722s1c1	-2.5	-1.9
PRKCE	NM_005400.x-591s1c1	-2.2	-3.5
PRKCE	NM_005400.x-1288s1c1	-2.0	-0.9

PRKCH	NM_006255.2-2285s1c1	-11.3	-9.2
PRKCH	NM_006255.3-481s1c1	-2.3	-3.5
PRKDC	NM_006904.6-1724s1c1	-2.3	-0.8
PRKDC	NM_006904.6-8611s1c1	-2.1	-1.5
PTK2	NM_005607.3-2779s1c1	-1.9	-2.8
PTK2	NM_005607.3-664s1c1	-1.8	-2.5
PTK2	NM_005607.x-2659s1c1	-1.0	-2.2
PTK2	NM_005607.3-817s1c1	-0.2	-2.0
RET	NM_020630.3-2529s1c1	-2.3	-0.5
RET	NM_020630.3-3378s1c1	-3.1	-2.6
RET	NM_000323.2-1587s1c1	-3.3	-2.2
RIOK2	NM_018343.1-1403s1c1	2.4	0.7
RIOK2	NM_018343.1-1082s1c1	3.0	1.1
RIPK1	NM_003804.x-1470s1c1	-4.7	-4.2
RIPK1	NM_003804.3-1266s1c1	-2.5	-2.0
RIPK1	NM_003804.3-2672s1c1	-2.4	-2.1
ROCK2	NM_004850.3-3765s1c1	-2.4	-2.6
ROCK2	NM_004850.3-583s1c1	-2.2	-0.2
ROCK2	NM_004850.3-5578s1c1	-0.7	-2.0
ROR2	NM_004560.x-3357s1c1	-4.5	-5.7
ROR2	NM_004560.2-1472s1c1	-3.3	-2.0
ROR2	NM_004560.2-3807s1c1	-2.0	-1.1
ROR2	NM_004560.x-1564s1c1	-0.2	-2.5
ROS1	NM_002944.x-3659s1c1	1.3	2.2
ROS1	NM_002944.x-294s1c1	1.5	2.2
RPS6KA5	NM_004755.x-677s1c1	-0.1	2.3
RPS6KA5	NM_004755.x-336s1c1	2.3	2.1
RPS6KB1	NM_003161.x-1501s1c1	1.6	2.5
RPS6KB1	NM_003161.x-1561s1c1	3.4	2.9
RYK	NM_002958.x-377s1c1	1.0	2.0
RYK	NM_002958.x-1526s1c1	0.8	2.2
SIK3	NM_025164.3-5245s1c1	2.1	0.5
SIK3	NM_025164.3-968s1c1	2.3	1.7
STK11	NM_000455.x-505s1c1	-3.5	-3.8
STK11	NM_000455.x-548s1c1	-1.9	-2.3
STK24	NM_003576.2-968s1c1	-4.6	-3.0
STK24	NM_003576.2-792s1c1	-2.2	-1.1
STK24	NM_003576.x-606s1c1	-1.1	-3.8
STK32B	NM_018401.1-400s1c1	-3.0	-2.0
STK32B	NM_018401.1-901s1c1	-2.3	-1.4
STK40	NM_032017.1-1244s1c1	-3.1	-1.6
STK40	NM_032017.1-2697s1c1	-3.0	-1.7
STRADA	NM_153335.4-693s1c1	-2.5	-3.1
STRADA	NM_153335.4-750s1c1	-1.0	-2.2
STRADB	NM_018571.4-397s1c1	-2.1	-2.9
STRADB	NM_018571.4-435s1c1	-2.1	-3.6

TGFBR1	NM_004612.2-758s1c1	-2.4	-1.7
TGFBR1	NM_004612.1-1463s1c1	-2.0	-0.5
TNIK	XM_039796.9-4033s1c1	1.6	2.1
TNIK	XM_039796.9-3935s1c1	-0.9	2.4
TSSK6	NM_032037.1-365s1c1	0.8	2.2
TSSK6	NM_032037.1-694s1c1	0.2	2.7
TWF2	NM_007284.3-1275s1c1	-2.0	-2.1
TWF2	NM_007284.3-897s1c1	-1.4	-2.2
TXK	NM_003328.1-1280s1c1	-2.1	-2.1
TXK	NM_003328.1-2159s1c1	-2.1	-1.6
TYK2	NM_003331.x-3209s1c1	-4.5	-3.7
TYK2	NM_003331.x-533s1c1	-4.4	-4.1
TYK2	NM_003331.x-4078s1c1	-3.0	-2.4
ULK2	NM_014683.2-780s1c1	-3.1	-0.6
ULK2	NM_014683.2-597s1c1	-2.0	-1.1
UNK	XM_038576.7-890s1c1	-2.6	-1.5
UNK	NM_016151.x-1186s1c1	-2.5	-2.2
UNK	NM_025164.3-2987s1c1	-2.2	-0.7
UNK	NM_025164.3-406s1c1	-1.7	-2.0
YES1	NM_005433.3-1351s1c1	2.0	1.6
YES1	NM_005433.3-1473s1c1	2.0	3.7
YES1	NM_005433.3-744s1c1	2.6	2.3
ZAP70	NM_001079.x-1820s1c1	-7.8	-6.8
ZAP70	NM_001079.x-2393s1c1	-3.1	-1.5

Table S3.

The gene names, shRNA clones, and robust z-scores for a small set of kinase hits identified, where at least two shRNAs for the specific kinase altered the YE210 DMR by ≥ 2 MAD (median absolute deviation), but with opposite directions. There were 15 kinases in total. These kinases were excluded from the follow-up analysis.

Gene name	shRNA clone	Early DMR	Late DMR
		Robust z score	robust z score
ALPK2	NM_052947.1-6185s1c1	-2.4	-3.0
	NM_052947.1-5452s1c1	2.9	1.4
AXL	NM_021913.x-1881s1c1	-3.1	-1.8
	NM_001699.x-1854s1c1	2.7	1.5
CDC2L2	NM_024011.1-155s1c1	-1.0	-2.0
	NM_024011.1-276s1c1	0.6	3.3
CDC2L5	NM_003718.x-5160s1c1	-6.4	-4.9
	NM_003718.x-3040s1c1	2.7	2.2
CDC42BPA	NM_014826.x-1153s1c1	-3.4	-3.3
	NM_006035.x-5307s1c1	2.7	1.8
CDK10	NM_003674.2-1496s1c1	-8.5	-4.0
	NM_052987.x-186s1c1	3.0	1.9
CDKL3	NM_016508.x-1442s1c1	-4.4	-4.7
	NM_016508.x-250s1c1	1.4	2.0
CSNK1E	NM_001894.4-2069s1c1	-3.8	-3.0
	NM_152221.x-895s1c1	1.5	2.7
EPHA1	NM_005232.2-2341s1c1	-3.2	-5.5
	NM_005232.2-159s1c1	2.2	1.4
FGFR3	NM_000142.x-1972s1c1	-5.5	-3.8
	NM_000142.x-3699s1c1	3.8	2.2
MYLK4	XM_373109.2-850s1c1	-2.0	-0.3
	XM_373109.2-1045s1c1	2.3	0.8
PKN1	NM_002741.x-525s1c1	-3.2	-0.7
	NM_002741.x-2064s1c1	2.0	1.9
PTK6	NM_005975.2-1506s1c1	-2.2	-2.8
	NM_005975.2-1064s1c1	2.6	2.2
RPS6KB2	NM_003952.2-371s1c1	-4.8	-4.1
	NM_003952.x-440s1c1	2.6	1.1
TTK	NM_003318.3-2515s1c1	-2.2	-2.1
	NM_003318.3-522s1c1	2.2	0.0

Table S1

Excel data summarizing DNA microarray data and genes that gave rise to intensity greater 100 RFU under at least one treatment condition and displayed at least two fold changes in expression level.